Mathematical Biosciences and Engineering

MBE, 19(3): 2381–2402.
DOI: 10.3934/mbe.2022110
Received: 28 August 2021
Revised: 07 November 2021
Accepted: 16 November 2021
Published: 04 January 2022

http://www.aimspress.com/journal/MBE

Research article

CNN-KCL: Automatic myocarditis diagnosis using convolutional neural network combined with k-means clustering

Danial Sharifrazi[1], Roohallah Alizadehsani[2], Javad Hassannataj Joloudari[3], Shahab S. Band[4,*], Sadiq Hussain[5], Zahra Alizadeh Sani[6,7], Fereshteh Hasanzadeh[7], Afshin Shoeibi[8], Abdollah Dehzangi[9,10], Mehdi Sookhak[11] and Hamid Alinejad-Rokny[12,13]

[1] Department of Computer Engineering, School of Technical and Engineering, Shiraz Branch, Islamic Azad University, Shiraz, IR
[2] Institute for Intelligent Systems Research and Innovation, Deakin University, Geelong, VIC 3216, AU
[3] Department of Computer Engineering, Faculty of Engineering, University of Birjand, Birjand, IR
[4] Future Technology Research Center, College of Future, National Yunlin University of Science and Technology 123 University Road, Section 3, Douliou, Yunlin 64002, TW
[5] System Administrator, Dibrugarh University, Assam 786004, IN
[6] Rajaie Cardiovascular Medical and Research Center, Iran University of Medical Sciences, Tehran, Iran
[7] Omid hospital, Iran University of Medical Sciences, Tehran, IR
[8] FPGA Laboratory, Faculty of Electrical Engineering, K. N. Toosi University of Technology, Tehran, IR
[9] Department of Computer Science, Rutgers University, Camden, NJ 08102, USA
[10] Center for Computational and Integrative Biology, Rutgers University, Camden, NJ 08102, USA
[11] Department of Computer Science, Texas A & M University at Corpus Christi, Corpus Christi, TX 78412, USA
[12] BioMedical Machine Learning Lab (BML), The Graduate School of Biomedical Engineering, UNSW Sydney, Sydney, NSW 2052, AU
[13] Health Data Analytics Program, AI-enabled Processes (AIP) Research Centre, Macquarie University, Sydney 2109, AU

* **Correspondence:** Email: shamshirbands@yuntech.edu.tw.

Abstract: Myocarditis is the form of an inflammation of the middle layer of the heart wall which is caused by a viral infection and can affect the heart muscle and its electrical system. It has remained

one of the most challenging diagnoses in cardiology. Myocardial is the prime cause of unexpected death in approximately 20% of adults less than 40 years of age. Cardiac MRI (CMR) has been considered a noninvasive and golden standard diagnostic tool for suspected myocarditis and plays an indispensable role in diagnosing various cardiac diseases. However, the performance of CMR depends heavily on the clinical presentation and features such as chest pain, arrhythmia, and heart failure. Besides, other imaging factors like artifacts, technical errors, pulse sequence, acquisition parameters, contrast agent dose, and more importantly qualitatively visual interpretation can affect the result of the diagnosis. This paper introduces a new deep learning-based model called Convolutional Neural Network-Clustering (CNN-KCL) to diagnose Myocarditis. In this study, we used 47 subjects with a total number of 98,898 images to diagnose myocarditis disease. Our results demonstrate that the proposed method achieves an accuracy of 97.41% based on 10 fold-cross validation technique with 4 clusters for diagnosis of Myocarditis. To the best of our knowledge, this research is the first to use deep learning algorithms for the diagnosis of myocarditis.

Keywords: myocarditis; diagnosis; convolutional neural network; biomedical machine learning, cardiac MRI; prediction

1. Introduction

Cardiovascular diseases (CVD) are among the most important causes of mortality around the world [1]. Atherosclerosis is the leading cause of CVD referring to the build-up of different substances including cholesterol and fat in and on the walls of the arteries. The flow of blood is constrained in such a situation which in turn affects the whole body. CVDs due to atherosclerosis include cerebrovascular disease (e.g. stroke), ischemic heart disease (e.g. heart attack), and hypertensive heart disease. Other CVDs embrace rheumatic heart disease, inflammatory heart disease, congenital heart disease, cardiac arrhythmias, and heart failure [1,2].

Inflammation of the heart muscles is clinically termed myocarditis [3]. In Figure 1, discrimination of normal and myocarditis affected heart can be seen. The inflammation of heart muscles is evident in myocarditis-affected heart as shown in Figure 1. The symptoms of myocarditis include chest pain or mild dyspnea. Common viral infections such as hepatitis B and C, parvovirus, and the recent one, COVID-19 may also cause myocarditis. Other specific forms of myocarditis include sarcoidosis, giant-cell myocarditis, hypersensitivity drug reactions, toxic or pathogens that may occur less commonly [4]. Patients that are diagnosed with myocarditis should be referred to the heart specialist for endomyocardial biopsy. The endomyocardial biopsy enables the clinicians to check the presence of premorbid in the patients of myocardial inflammation. Myocardial is the prime cause of unexpected death approximately 20% in adults less than 40 years old [5]. Although it had been centuries since the recognition of this enigmatic disease, effective treatment strategies are yet to develop because of several issues such as insensitivity to diagnostic tests, complex relations between maladaptive and adaptive immune responses [4]. A recent development in the genetic basis of immune-mediated heart disease and studies in animals provided key information in treating the disease.

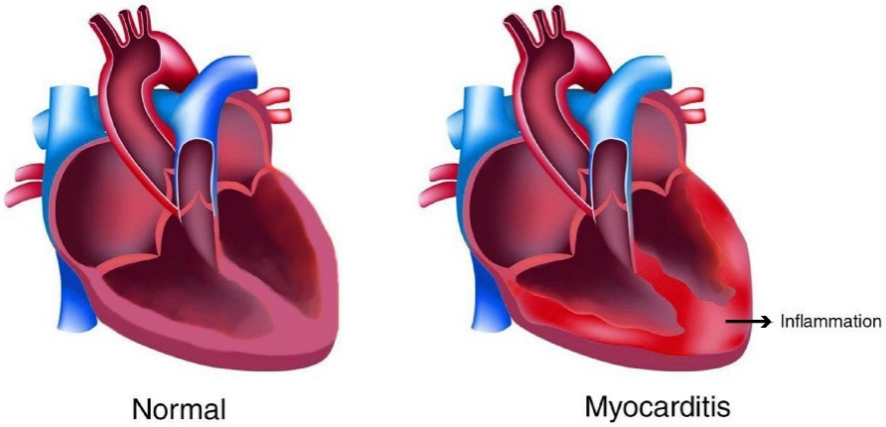

Figure 1. Demonstration of myocarditis (on the right) and normal heart (on the left). As shown here, the inflammation of the heart muscles is evident in the myocarditis-affected heart.

Early detection of heart diseases is crucial for decreasing the mortality rate [6]. The screening methods such as electrocardiograms, echocardiograms, or magnetocardiogram help physicians diagnose the disease at an early stage. However, factors such as fatigue and excessive workload of the physician as well as other factors such as the presence of various noises in the images, or the presence of a mass or lesion that are not visible can cause misdiagnosis [7]. To address this problem, computer-aided diagnosis (CAD) can help clinicians in diagnosing the diseases in their early stages [8]. Using CAD as a machine learning methodology is deployed to predict and analyses different disease-related issues [9]. One of the most advanced algorithms for analyzing large numbers of images collected from patients is the deep learning-based method. In fact, for deep learning-based methods, the more the input data increases, the more they become accurate and efficient [10].

To the best of our knowledge, there is no scientific literature related to deep learning-based studies on the detection and diagnosis of myocarditis disease. This is the first step towards such a study. We, therefore, systematically reviewed the literature based on cardiomyopathy oriented diseases. The rest of the paper is organized as follows: Section 2 describes the literature review; Section 3 presents the Z-Alizadeh Sani myocarditis dataset; Section 4 represents the method while Section 5 describes experimental results which are followed by Section 6 that presents the conclusion and future work.

2. Literature review

Baeßler et al. [11] examined whether machine learning-based techniques might be utilized for the recognition of myocardial tissue alterations in hypertrophic cardiomyopathy (HCM) on T1-weighted non-contrast cardiac magnetic resonance (CMR) images using texture analysis (TA). In this study, texture feature selection and step-wise dimension reduction were explored for feature selection and identification of myocardial tissue alterations on non-contrast T1-weighted CMR images in HCM patients.

In another study, Ovreiu and Simon [12] investigated the diagnosis of cardiomyopathy in its two common forms: hypertrophic and dilated via *P* wave features. They applied a novel evolutionary technique dubbed biogeography-based optimization (BBO) and developed a neuro-fuzzy network.

They demonstrated that cardiomyopathy could be successfully diagnosed by applying a neuro-fuzzy model. Later Ali et al. presented a computerized framework for the detection of cardiomyopathy diseases utilizing a multilayered perceptron (MLP) neural network [13]. In this study, the high-frequency noise removal method was employed using moving and median average filters at the preprocessing stage.

More recently Alis et al. [14] exploited a machine learning approach for texture feature analysis of cardiac magnetic resonance imaging (MRI) for examining the incidence of ventricular tachyarrhythmia (VT) in hypertrophic cardiomyopathy patients. Similarly, Borkar et al. [15] proposed a machine learning approach for the automatic detection of Atrial Septal Defect (ASD) and dilated cardiomyopathy (DCM) diseases. Their dataset comprised of the ultrasound videos of DCM, ASD, and normal cases. In another study, Sengupta et al. [16] designed a machine learning algorithm based on an associative memory classifier using echocardiographic and clinical records of 44 patients with restrictive cardiomyopathy and 50 patients with constrictive pericarditis. To discriminate constrictive pericarditis from restrictive cardiomyopathy, they normalized the speckle tracking echocardiography images concerning 47 controls with no structural heart disease and evaluated the diagnostic area under the ROC curve of the associative memory classifier.

At the same time, Begum et al. [17] developed an automated diagnostic system for cardiomyopathy disease using feed-forward backpropagation neural network and SVM classifiers. They utilized an online PTB diagnostic ECG database and preprocessed it for baseline correction and noise cancellation. They then proposed four time-based features and classified them using artificial neural networks and SVM [18]. More recently, Green et al. [19] studied the echocardiograms and photoplethysmography data from a control cohort of 64 healthy volunteers and 19 HCM patients with left ventricular outflow tract obstruction (oHCM). In another study, Tsai and Kojima [20] utilized four texture features of ultrasonic images for heart disease classification. Their proposed method took as input the heart images that measured texture features by generating a gray-level co-occurrence matrix.

More recently, Narula et al. [21] examined the potential for a machine learning system that integrated speckle-tracking echocardiographic recordings for discrimination of HCM from physiological hypertrophy seen in athletes (ATH). Similarly, Rahman et al. [22] proposed an HCM patient classifier utilizing standard 12-lead and 10-seconds ECG signals. They derived 504 temporal and morphological features including both newly-developed and commonly used ones from ECG signals for heartbeat classification.

Recently, Shao et al. [23] examined whether TA parameters on magnetic resonance T1 mapping could be applied for the diagnosis of DCM. In this study, modified look-locker inversion recovery (MOLLI) sequence at a 3.0 T MR scanner was used to acquire T1 maps. The epicardium and endocardium were strained on the short-axis slices of the T1 maps by a skilled radiologist. Most recently, Capture et al. [24] performed plasma proteomics and exploratory myocardial screens and consequently devised a multiplexed targeted liquid chromatography-tandem/mass spectrometry-based assay to examine 26 peptide biomarkers to recognize novel plasma biomarkers for patients with HCM.

Ali et al. [25] predicted heart disease utilizing a smart healthcare system applying feature fusion and ensemble deep learning methodologies. Conventional methods fail to diagnose heart diseases as they cannot tackle high-dimensional data. Hence, a smart framework using deep learning strategies is effective in such cases. In different electronic health records (EHR) from hospitals, there are lots of features, and the distribution of such features is also very unbalanced. Baccouche et al. [26] devised an ensemble framework based on deep learning to handle the unbalanced heart disease dataset issue.

A substantial amount of human effort is needed as machine learning approaches rely on rules and dictionaries and the integration of data-driven and knowledge-driven techniques. The simplicity of deep learning models comes to the rescue on detection of heart-related diseases and their risk factors compared to feature-engineered hybrid methods. The authors [27] designed a deep learning architecture from EHR records to evaluate the risk factors for heart disease. Early detection of heart-related issues is possible when heart disease systems are integrated into the Internet of Medical Things. Su et al. [28] utilized deep learning methods on the internet of medical things for the detection of valvular heart disease. The author [29] proposed deep learning modified neural network (DLMNN) using IoT for assisting heart disease diagnosis and this patient monitoring approach achieved a competitive outcome. Morris et al. [30] introduced a deep learning method to diagnose congenital heart disease in the fetus, the most lethal and common birth defect. Correct prediction of heart disease can save lives while incorrect one can be fatal. The authors [31] applied a deep learning approach to predict the occurrence of heart disease in diabetic patients. They used two models-gated recurrent unit (GRU) and long short-term memory (LSTM). GRU outperformed the LSTM in such prediction. Bharti et al. [32] integrated machine learning techniques with deep learning models to predict heart disease. They used the UCI Machine Learning Heart Disease dataset and their technique yielded promising accuracy. The authors [33] proposed an echocardiography-based mortality deep learning prediction model for heart patients. They validated their model using the areas under the receiver operating characteristic curve (AUROC) and showcased superior performance. Sharma et al. [34] deployed a deep neural network (DNN) model for the prediction of heart disease and they observed that Talos optimization recorded state-of-the-art performance. Poplin et al. [35] predicted the cardiovascular risk factors from analyzing retinal images such as major adverse cardiac events, systolic blood pressure, smoking status, gender, and age. Hence, deep learning approaches are crucial in diagnosing and detection of various heart diseases from different sources related to patients.

As is highlighted in the literature review, no deep learning-based method has been used for diagnosing myocarditis so far. In this study, we propose a new deep learning model (called CNN-KCL) that is build based on the combination of deep convolutional neural network (CNN) and k-means clustering to solve this problem. Our results demonstrate that CNN-KCL can significantly enhance the prediction performance compared to previous studies found in the literature.

3. Z-Alizadeh Sani myocarditis dataset

Cardiac MR Imaging is considered the noninvasive and diagnostic golden standard of myocarditis in the absence of biopsy. CMR provides the possibility of anatomical and functional imaging and accurate assessment of the heart. In this respect, its ability for tissue characterization is even more important [36]. Three diagnostic targets for the three recommended Cardiac MRI criteria are myocardial edema, hyperemia/capillary leak, and scar which is known as Lake Louise Criteria (LLC) [37]. The existence of contrast enhancement (CE-GD) affirms myocardial injury (i.e. scar, fibrosis) while T2-weighted images show interstitial edema, known as an integral part of the inflammatory response. The pre-and post-contrast T1-Weighted image indicates the presents of hyperemia/capillary leak in myocardial tissue. The LLC has been accepted beyond clinical criteria and Endomyocardial biopsy. Two out of three "Lake Louise Criteria" have 80.0% accuracy for a correct diagnosis of acute myocarditis [38]. In this study, we developed a model to diagnose myocarditis based on three indexes of Lake Louise Criteria (LLC).

3.1. CMR imaging protocols

This study was performed from September 2018 to September 2019 at the CMR department of OMID hospital in Tehran, IRAN[1]. The total number of images in this study is 98,898 including 37,564 images from healthy individuals and 61,334 images from individuals with Myocarditis issues. The study was approved by the local ethical committee of the OMID hospital. CMR examination was performed using a 1.5-T system (MAGNETOM Aera Siemens, Erlangen Germany) [39]. All patients were scanned with dedicated body coils in the standard supine position. The CMR protocols are as follows:

We performed CINE-segmented images and pre-contrast T2-weighted (trim) images in short and long-axis views. Pre contrast T1-Weighted relative images were acquired in axial views of the myocardium. Immediately after gadolinium injection (DOTAREM 0/1 mmol/kg), the T1-weighted relative sequence was repeated and after 10-15 minutes, Late Gadolinium Enhancements (LGE-high-resolution PSIR) sequences in short and long-axis views were performed. Table 1 shows the parameters and details of CMR sequences. In addition, the main characteristics of our dataset are presented in Table 2.

Table 1. Z-Alizadeh Sani myocarditis dataset description.

Protocols & Parameters	TE (ms)	TR (ms)	Segment	Slice thickness (mm)	Concatenation and Slice number	NEX	Breath-hold time (s)
CINE_segmented (true FISP) Long Axis (LAX):	1.15	33.60	15	7	3	1	8
CINE_segmented (true FISP) Short Axis (SAX):	1.11	31.92	15	7	15	1	8
T2-Weighted (TIRM) LAX, pre-contrast	52	800	Non-cine	10	3	1	9
T2-Weighted (TIRM) SAX, pre-contrast	52	800	Non-cine	10	5	1	10
T1 Relative-Weighted TSE (Trigger)- AXIAL-dark blood pre- and post-contrast	24	525	Non-cine	8	5	1	7
Late-GD Enhancement LGE (high-resolution PSIR) SAX and LAX	3.16	666	Non-cine	8	1	1	7

Note: TE: Time Echo, TR: Time Repetition, Segment: Numbers of frames (Segmented acquisition to produce a series of images that can be displayed as a movie of cardiac function (cine)), Slice Thickness: How thick the slices are, Concatenation: Distribution of the slices to be measured over multiple TR, NEX: Number of Excitations (How many times each line of k-space data is acquired during the scan), Breath-hold time: Duration of time that the patient should hold his/her breath to avoid chest motion artifacts.

[1] https://www.kaggle.com/danialsharifrazi/cad-cardiac-mri-dataset

Table 2. Some of the characteristics of the Z-Alizadeh Sani myocarditis dataset.

	(Mean ± STD) of			
	Age (Year)	Height (cm)	Weight (Kg)	Number
Myocarditis	39.51 ± 18.77	174.67 ± 6.13	77.70 ± 15.14	32
Normal	37.27 ± 18.10	167.10 ± 6.02	68.27 ± 16.67	15

4. Methods

In this section, we present our proposed method in detail.

4.1. Background knowledge

In this study, we use convolutional neural network (CNN) and k-means clustering to build our proposed model. Here, CNN is selected as one of the most powerful methods among deep learning algorithms for image analysis [40−42]. K-means is also selected because of heterogeneity among our input data. Having different viewpoints, light conditions, etc. have a negative impact on the classification performance. Hence, before classification, we use the k-means algorithm to cluster the images. In this way, similar images are categorized in the same cluster which potentially helps in enhancing the performance and overcoming heterogeneity in our input data.

4.1.1. Convolutional neural network (CNN)

One of the well-known deep learning techniques for image processing is convolutional neural network (CNN) that takes an image as input, allocates importance (biases and learnable weights) to different objects/aspects in the image, and then classify them [43]. CNN requires much lower pre-processing compared to the other deep learning architectures. Generally, filters are hand-engineered in primitive methods while CNN can learn these characteristics/filters. The connectivity pattern of neurons in the human brain and the architecture of CNN are analogous. CNN is developed based on the organization of the visual cortex. A CNN is comprised of an input layer, multiple hidden layers, and an output layer. The hidden layers of CNN are typically created with convolutional layers that convolve with others [44]. The activation function is usually a rectified linear units (ReLU) layer and additional convolutions such as normalization layers, fully connected layers, and pooling layers are consequently followed [45]. There are various architectures of CNNs that are extensively used in the deep learning domain. Some of such architectures are LeNet [46], AlexNet [47], VGGNet [48], GoogleNet [49], and ResNet [50]. CNN is widely used in many different areas of research including computer vision, medical image analysis, recommendation system, financial time series, natural language processing, image, and video recognition, and classification [51,52]. CNN has been applied successfully in detection and diagnosis of various diseases using various image modalities [40,44,53–57].

4.1.2. K-means clustering

K-means clustering is one of the popular and simplest unsupervised techniques used in the machine learning domain [58]. It is based on vector quantization that aims to partition n observations into k clusters. Each observation belongs to a cluster with the nearest mean value (cluster centroid or cluster centers). The Euclidean distance (or any other distance metrics) is usually utilized to generate k groups [59]. Each item is categorized to its closest mean and the mean's coordinates are updated as the averages of the items categorized in that cluster so far.

4.2. Proposed method

In this section, the proposed method is described in two parts. At first, the CNN-KCL scheme and then its structure is explained in detail.

4.2.1. Proposed CNN-KCL scheme

The block diagram of the proposed method namely convolutional neural network-clustering (CNN-KCL) is shown in Figure 2, which includes the steps of data entry, clustering, classification, and final prediction.

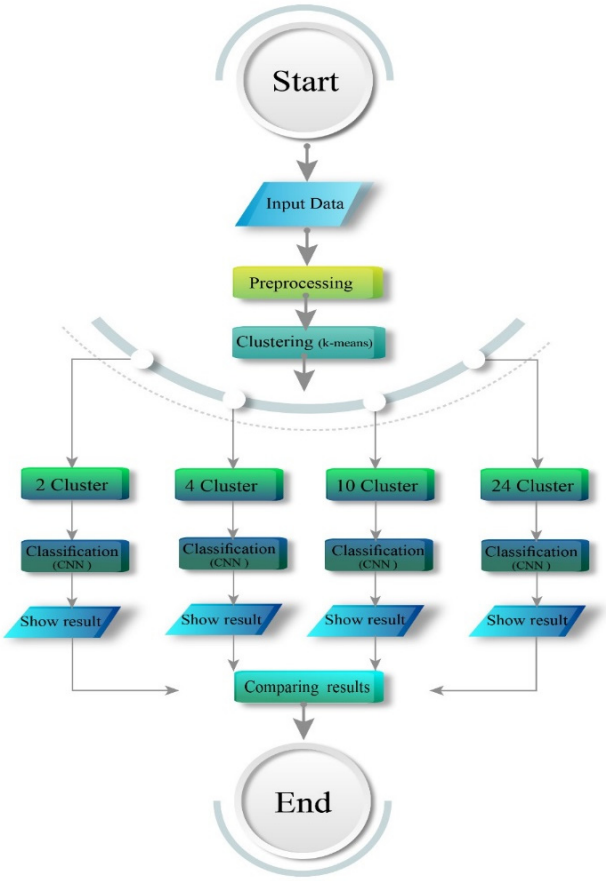

Figure 2. The block diagram of the proposed CNN-KCL method.

According to Figure 2, the implementation steps are shown briefly:

- Step 1: In the first step, the proposed dataset is entered into the system.
- Step 2: The second step is related to the initial pre-processing. All dataset images are on a gray level. Hence, there is no need to delete the image channels. Dataset images are available in a variety of sizes. For this purpose, all images are resized to a size of 100 × 100. After resizing the images in the data pre-processing step, the image normalization operation is performed. Normalization of images transforms the light intensity of all image pixels to the range of zero and one (0 and 1).
- Step 3: Due to the great variety of image sections, clustering is used in this step. There are different methods for clustering data. In this research, the k-means method is used to cluster images. It is important to note that the k-means algorithm is not capable of clustering two-dimensional images. For this reason, all images are reshaped into the vector of pixels, and then these are used in the k-means algorithm.
- Step 4: In this step, the data is divided into 2, 4, 10, and 24 clusters by the k-means algorithm.
- Step 5: In this step, the data are classified using CNN separately. Convolution layers are used for feature extraction and fully connected layers act as classifiers in this network.
- Step 6: In step 6, the results of the classification of 2, 4, 10, and 24 clusters are displayed separately.
- Step 7: Finally, the results of the classification of clustered images performed by k-means and CNN algorithms are compared.

In this study, we have studied different values for K starting from 2 to find the optimal number of clusters, experimentally. Initially, the Z-Alizadeh Sani myocarditis dataset was given to the CNN-KCL model with two classes of healthy and Myocarditis (2 clusters). Due to a great variety in the employed dataset and the existence of images taken from different viewpoints, the initial accuracy of CNN-KCL was low. For this reason, the data was divided into more clusters to represents the data with a more distinctive pattern. To test other values for K, we divided each healthy and sick people into 2 clusters (a total of 4 clusters (K = 4)). This way, input images should be classified by CNN-KCL into 4 classes. We also increased the number of clusters to 10 (5 clusters for sick people and 5 clusters for healthy people). As a result, a total of 10 clusters or 10 classes (K = 10) were created to identify healthy and sick people as the output of CNN-KCL. Finally, the number of clusters was increased to 24 (K = 24). An input image is classified as healthy if it is categorized in one of the healthy clusters. The performance was tested based on 10 fold-cross validation technique (i.e. 90% of the data for training and 10% of the data for testing). However, the results almost monotonically decreased. As the result, at K = 24 which produced the lowest results, we stopped increasing the number of clusters.

4.2.2. Recommended CNN-KCL architecture

The proposed CNN-KCL architecture is shown in Figure 3. CNN-KCL includes input layers, convolution (32 kernels), Maxpooling (2 × 2), Dropout, re-convolution layers (64 kernels), Maxpooling (2 × 2), and Dropout. It also has the Flatten layer, fully connected, and the dropout layer, and finally the desired output. The list of hyperparameters optimization of the proposed CNN-KCL is described in detail in Table 3.

Table 3. The list of hyperparameters settings of the proposed method.

Number of Kernels from first to the third	Size of the convolution kernels	Size of the max-pooling kernels	Number of neurons in the Fullv Connected	Number of neurons in the output laver	Size of the Dropout	Number of batch size	Number of epochs	Value of validation data	Optimizer function	Activator function	Output layer classifier for the 2 clusters	Output layer classifier for more than 2 clusters
32, 64, and 64	3 * 3	2 * 2	100	4, 10 and 24	0.2	32	70	0.3 and 0.2	Adam	ReLU	sigmoid	SoftMax

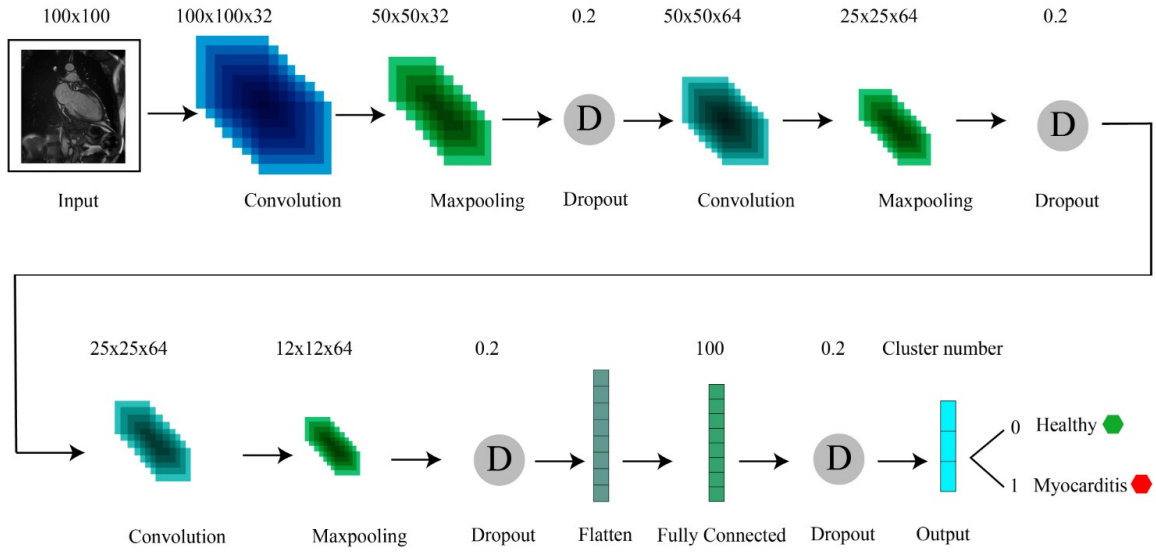

Figure 3. The general architecture of CNN-KCL.

According to Figure 3, images are reshaped to a size of 100 × 100 into the CNN network. As the first part of the network, a convolution layer with a 3 × 3 kernel size, a Max-pooling layer with a 2 × 2 kernel size, and a dropout layer with a size of 0.2 has been selected. In this network, the convolution layer is used to extract the feature from the dataset. The dropout layer is used to randomly remove a number of neurons to avoid overfitting in the network. The combination of these three layers with the activation function on CNN is usually referred to as one layer. The proposed CNN network consists of three layers with the mentioned features. The numbers of filters in the first, second, and third convolution layers are 32, 64, and 64, respectively. After passing the data through these three layers, the Flatten layer is used to change the form of the data from two-dimensional to one-dimensional mode. Then, the Fully Connected layer is used to classify the network. After the fully connected layer, the dropout layer is used again to avoid the network overfit. As the output layer, there is a vector with the number of neurons equal to the number of clusters, i.e., 2, 4, 10, and 24.

5. Experimental results

In this section, the results of applying the proposed algorithm on the Z-Alizadeh Sani myocarditis dataset are reported. We used Python programming language and Tensorflow to implement CNN-KCL. In each of the K values (2, 4, 10, and 24), CNN-KCL networks were executed and the results were obtained based on 10 fold-cross validation technique and shown in Figures 4 and 5. The figures represent Accuracy [60–62] and LOSS [63–65].

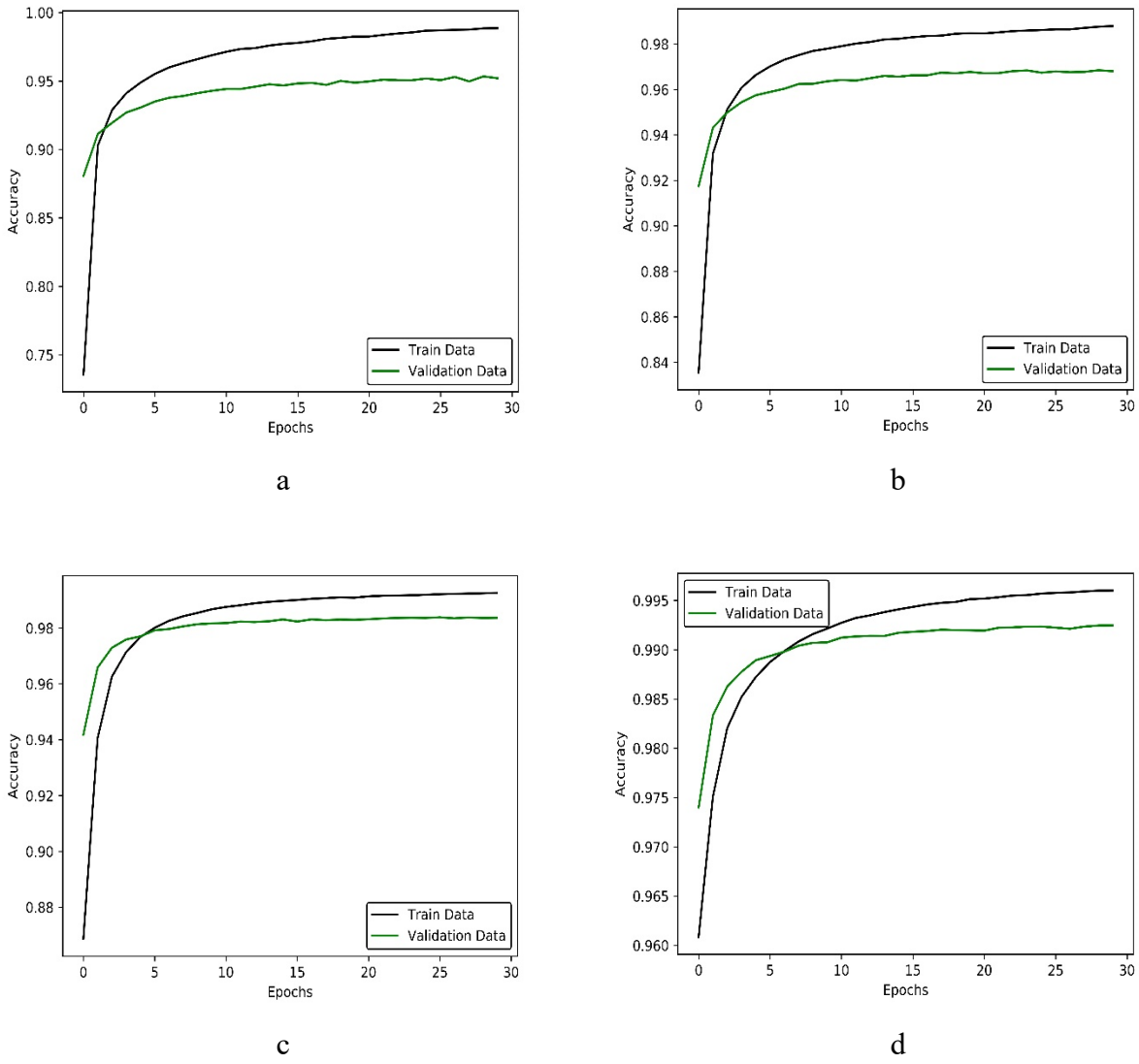

Figure 4. Accuracy of CNN-KCL for different numbers of clusters based on 10 fold cross-validation technique. a) 2 clusters b) 4 clusters. c) 10 clusters d) 24 clusters.

Figure 4 shows the accuracy based on 10 fold-cross validation technique. In each of these two figures, the results with 2, 4, 10, and 24 clusters are shown and the blue and orange lines represent the training and validation process over 30 epochs, respectively. In Figure 4, with 2 clusters, the CNN-KCL network is not well trained and had low accuracy. While in 4-cluster, 10-cluster, and 24-cluster modes, the training and validation processes are almost pretty similar with the same accuracy. As

shown in these figures, the best results are achieved using CNN-KCL while the number of clusters (K) is set to 4.

Figure 5 shows the loss of CNN-KCL for a different number of clusters. As shown in Figure 5, in the case of 2 clusters, the loss increases dramatically, and in the cases of 4, 10, and 24 clusters, the loss decreases based on 10 fold cross-validation technique. In the case of 4 clusters, we observe the least loss. We also observe similar results in 4, 10, and 24 clusters in Figure 5.

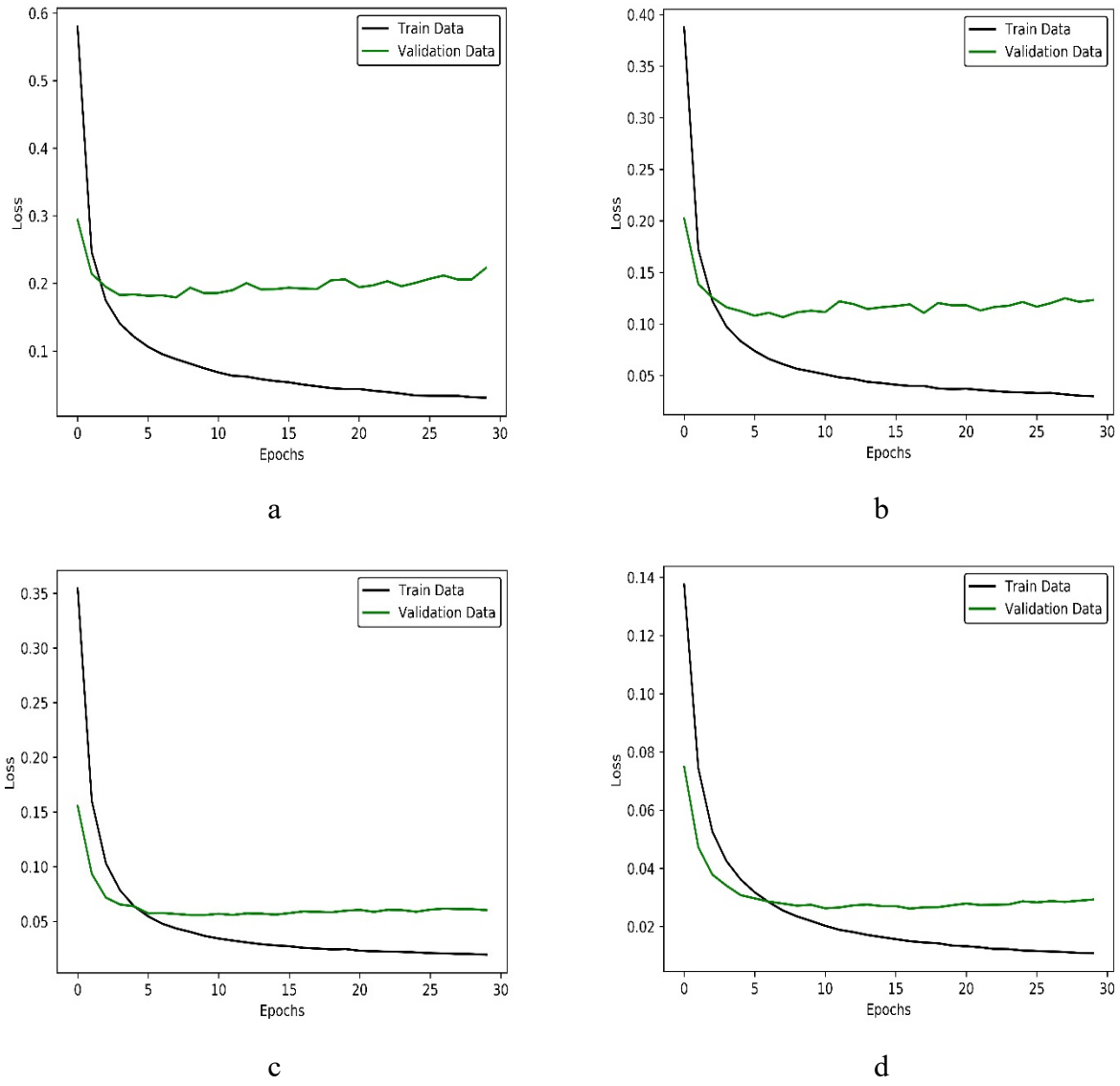

Figure 5. Loss of CNN-KCL for a different number of clusters based on 10 fold cross-validation technique. a) 2 clusters. b) 4 clusters. c) 10 clusters. d) 24 clusters.

According to Table 4, we investigated various evaluation criteria including precision, accuracy, recall, specificity, F1-Score, and AUC. When there are 2 clusters, by dividing the data set into 90% for training and 10% for testing or 10-fold cross-validation technique, the values of accuracy, precision, recall, specificity, F1-score, and AUC are 95.24, 94.6, 92.7, 96.78, 93.8, and 94.75%, respectively.

Meanwhile, the best performances are achieved when the CNN-KCL algorithm is used while K is set to 4 in the k-means algorithm.

Table 4. The achieved classification results using CNN-KCL based on a 10-fold cross-validation technique for the different number of clusters.

Number of clusters	Accuracy (%)	Precision (%)	Recall (%)	Specificity (%)	F1-score (%)	AUC (%)
2 clusters	95.24	94.6	92.7	96.78	93.8	94.75
4 clusters	97.41	97.6	95.7	98.56	96.5	97.05
10 clusters	97.04	97.8	94.5	98.71	95.9	96.51
24 clusters	96.98	98.3	93.7	99	96.1	96.34

To investigate the effectiveness of CNN-KCL, we compare it with several state-of-the-art traditional machine learning models such as bayesian network (BN) [18,66,67], decision tree (DT) [67−69], logistic regression (LR) [67,70,71], and random forest (RF) [67,71,72]. The above methods are described below.

1) Bayesian network

The BN classifier is the probability-based multiclass method and maximum likelihood computing. In other words, the NB classifier generates a conditional probability model, based on the use of the Bayes theorem that predicts the probability of a patient. Indeed, the supervised learning classifier accepts that the existence of a specific feature in a class is irrelevant to the existence of other features.

2) Decision tree

The next supervised learning classifier is the rule-based decision tree that is utilized for medical cases. This classifier is with a tree structure, comprising a root node, branches, and leaf nodes. Using the DT classifier, the dataset is separated into categories according to low entropy measures. It separates the dataset into two or more homogeneous sets. This is done based on the most important independent variables to make as discrete categories as conceivable. The decision tree achieves effective results with good accuracy.

3) Logistic regression

The LR classifier is a probabilistic binary classification method. This classifier is amplified by the correlation amid the dependent and independent variables through a linear separating line. The best separating line is named the regression line.

4) Random forest

The RF classifier is a non-probabilistic multiclass classification method. This RF method is an ensemble method, incorporating the predictions returned by a large number of trees of decision trees through the utilization of a bootstrap aggregation method. Every decision tree within the ensemble is created by frequently splitting the training dataset into subsets, to increase the monotony of the subsets. Furthermore, the forest selects the classification considering the most votes for entirely the trees.

As it is specified earlier, to the best of our knowledge, CNN-KCL is the first deep learning-based method that has been used for this task. The results of this comparison are illustrated in Table 5. As shown in Table 5, CNN-KCL outperforms all the other traditional machine learning models. CNN-

KCL is the first machine learning model to achieve over 90% in terms of Accuracy, Precision, and Recall. It also achieves over 0.9 F1-score.

Table 5. The comparison results between the proposed CNN-KCL with 4 clusters and some other classification methods through the 10-fold cross-validation technique.

Methods	Accuracy (%)	Precision (%)	Recall (%)	Specificity (%)	F1-score (%)	AUC (%)
BN	54.11	44	77.3	39.94	56.2	58.59
DT	91.99	89.1	90	93.37	89.4	91.55
LR	89.52	86.9	85.1	92.2	86.1	88.68
RF	94.4	92.9	92.3	95.7	92.7	94
CNN-KCL	97.41	97.6	95.7	98.56	96.5	97.05

Table 6. The accuracies and STD based on the 10-fold cross-validation.

No. Fold	STD for train data	STD for test data	Accuracy of CNN	Accuracy of CNN-KCL (4 clusters)	Accuracy of CNN-KCL (10 clusters)	Accuracy of CNN-KCL (24 clusters)
1	53.1117	52.9548	0.9506548888212001	0.9619250685348767	0.8192913080123563	0.9217518051816359
2	53.0759	53.2771	0.9548177479947203	0.6729617220022337	0.8573154699973061	0.9270188356247127
3	53.0820	53.2231	0.9514163874928655	0.6775560970656932	0.8766169213069 9	0.9181389158202223
4	53.0538	53.4748	0.9528838342810723	0.7997309098294007	0.8094333984036449	0.9219934845919723
5	53.0985	53.0749	0.9514622258326564	0.8012540617384241	0.8315800248753433	0.9215788493109955
6	53.0937	53.1180	0.9462835093419983	0.5053818034118602	0.8023659715702822	0.9209399717692724
7	53.1087	52.9824	0.9520207148659626	0.5065241673436233	0.8103980613277755	0.9300577294332627
8	53.1396	52.7029	0.9565393988627132	0.6740454914219296	0.8223497238128191	0.9263640860538963
9	53.1058	53.0085	0.9535438667749797	0.5066764825345248	0.8931458209899265	0.9224969726282828
10	53.0914	53.1387	0.9542038992688887	0.9677853371242892	0.8318643470685914	0.9238339626237109

According to the results shown in Table 5, our method performance is in the first rank. RF, SVM, and LR are in the next ranks, respectively. DT and BN are at the end of this list.

In addition, the accuracies and standard deviation (STD) have been achieved based on the 10-fold cross-validation that is described in Table 6.

For more comparison, the results of statistical tests were obtained for methods. These tests have been assigned in Table 7.

Table 7. The results of statistical tests for methods.

CNN-KCL (4 clusters) and CNN (without clustering)	t_statistics: -4.435183828438278 degree of freedom: 18 critical value: 1.7340636066175354 p_value:0.0003196116199775112
CNN-KCL (4 clusters) and CNN-KCL (10 clusters)	t_statistics: -2.283893609489031 degree of freedom: 18 critical value: 1.7340636066175354 p_value:0.03474105191887733
results for CNN-KCL (4 clusters) and CNN-KCL (24 clusters)	t_statistics: -3.9105542487284772 degree of freedom: 18 critical value: 1.7340636066175354 p_value:0.0010250233862463265

6. Conclusions and future works

Myocarditis which remains one of the most challenging diagnoses in cardiology can affect the heart muscle and its electrical system. The most common cause of myocarditis is viral infection but other potential causes include Bacteria, Parasites, Fungi, Medications, or illegal drugs that might cause an allergic or toxic reaction, chemicals, or radiation [73]. Patients might present with a wide variety of symptoms like palpitations, dizziness, or syncope, serious ventricular arrhythmia, and angina-like chest pain [4]. Sudden cardiac death and acute coronary syndrome in healthy young adults can be caused by heart failure or severe arrhythmia [74].

Nowadays, the application of machine learning techniques to identify uncover hidden healthcare patterns has been increased, dramatically. Thanks to the advent of technology, diagnostic possibilities have expanded and improved but there is still room for additional modifications and improvements [75]. Endomyocardial biopsy (EMB) as the invasive gold standard for diagnosis of myocarditis is subject to sampling error, false negative, false-positive results, procedural risks, or lack of local expertise therefore due to these limitations is infrequently performed [76]. Among non-invasive methods, Electrocardiogram (ECG) and echocardiography are the primary diagnostic tools for heart diseases which are applicable for excluding other causes of cardiomyopathy. They can help to document disease development because temporal changes in systolic function, chamber size, and thickness can be evaluated regularly. However, they do not provide determined signs for myocarditis [77]. Cardiac MRI (CMR) has been considered a noninvasive and golden standard diagnostic tool for suspected myocarditis and plays an indispensable role in diagnosing various

cardiac diseases. CMR provides the possibility of anatomical and functional imaging and accurate assessment of the heart. However, in this respect what is more important is its ability of tissue characterization [36,75].

Based on our experimental results, the convolutional neural network demonstrates promising performance for detecting and classifying images. However, to the best of our knowledge, no studies have used deep learning-based methods to diagnose myocarditis so far. We also used the k-means clustering method to reduce the impact of heterogeneity among the input samples. Here, at first, we used the Elbow method (explained in detail in Appendix) to identify the optimal number of clusters [78]. However, in our case, this method was not able to provide us with the best results. Therefore, we used an alternative experimental approach to identify the optimal number of clusters for the k-means algorithm. In this study, clustering the data was used to overcome heterogeneity in the input data. After that, a novel hybrid CNN-KCL method was used to diagnose and classify myocarditis on the Z-Alizadeh Sani myocarditis dataset. The data set was divided into 90% for training and 10% testing based on a 10-fold cross-validation technique. We demonstrated our results using various evaluation criteria including accuracy, precision, specificity, F1-score, recall, and AUC. As shown in Table 4, CNN-KCL with K = 4 achieved 97.41, 97.6, 98.56, 96.5, 95.7, and 97.05% in terms of accuracy, precision, recall, specificity, F1-score, and AUC, respectively. In addition, we compared our proposed method with the most popular traditional classification algorithms (Table 5). The result of this comparison demonstrated that CNN-KCL can significantly outperform other traditional machine learning algorithms for this task.

As for future works, we aim at using semi-supervised methods, reinforcement learning, and supervised methods such as recurrent neural networks (RNNs) to enhance the prediction performance. We also aim at using explainable AI and case-based reasoning (CBR).

Conflict of interest

The authors declare no competing financial and non-financial interests.

Coda and dataset availability

The scripts and dataset are available at: https://www.kaggle.com/danialsharifrazi/myocardit-dataset-code.

References

1. J. H. Joloudari, E. H. Joloudari, H. Saadatfar, M. Ghasemigol, S. M. Razavi, A. Mosavi, et al., Coronary artery disease dagnosis; ranking the significant features using a random trees model, *Int. J. Environ. Res. Public Health*, **17** (2020), 731. https://doi.org/10.3390/ijerph17030731.
2. M. Aazam, E. N. Huh, Fog computing micro datacenter based dynamic resource estimation and pricing model for IoT, in *2015 IEEE 29th International Conference on Advanced Information Networking and Applications*, IEEE, (2015), 687–694. https://doi.org/10.1109/AINA.2015.254.
3. W. Cooper, S. Hernandez-Diaz, P. Arbogast, Myocarditis, *N. Engl. J. Med.*, **354** (2006), 2443−2451. https://doi.org/10.1056/NEJMoa055202.

4. L. A. Blauwet, L. T. Cooper, Myocarditis, *Prog. Cardiovasc. Dis.*, **52** (2010), 274–288. https://doi.org/10.1016/j.pcad.2009.11.006.
5. A. M. Feldman, D. McNamara, Myocarditis, *N. Engl. J. Med.*, **343** (2000) 1388−1398. https://doi.org/10.1056/NEJM200011093431908.
6. R. Alizadehsani, M. H. Zangooei, M. J. Hosseini, J. Habibi, A. Khosravi, M. Roshanzamir, et al., Coronary artery disease detection using computational intelligence methods, *Knowl. Based Syst.*, **109** (2016), 187–197. https://doi.org/10.1016/j.knosys.2016.07.004.
7. E. Nasarian, M. Abdar, M. A. Fahami, R. Alizadehsani, S. Hussain, M. E. Basiri, et al., Association between work-related features and coronary artery disease: A heterogeneous hybrid feature selection integrated with balancing approach, *Pattern Recognit. Lett.*, **133** (2020), 33–40. https://doi.org/10.1016/j.patrec.2020.02.010.
8. R. Alizadehsani, M. Roshanzamir, M. Abdar, A. Beykikhoshk, A. Khosravi, S. Nahavandi, et al., Hybrid genetic-discretized algorithm to handle data uncertainty in diagnosing stenosis of coronary arteries, *Expert Syst.*, 2020. https://doi.org/10.1111/exsy.12573.
9. R. Alizadehsani, M. Roshanzamir, M. Abdar, A. Beykikhoshk, M. H. Zangooei, A. Khosravi, et al., Model uncertainty quantification for diagnosis of each main coronary artery stenosis, *Soft Comput.*, **24** (2020) 10149−10160. https://doi.org/10.1007/s00500-019-04531-0.
10. H. Greenspan, B. Van Ginneken, R. M. Summers, Guest editorial deep learning in medical imaging: overview and future promise of an exciting new technique, *IEEE Trans. Med. Imaging*, **35** (2016), 1153–1159. https://doi.org/10.1109/TMI.2016.2553401.
11. B. Baeßler, M. Mannil, D. Maintz, H. Alkadhi, R. Manka, Texture analysis and machine learning of non-contrast T1-weighted MR images in patients with hypertrophic cardiomyo pathy−Preliminary results, *Eur. J. Radiol.*, **102** (2018), 61–67. https://doi.org/10.1016/j.ejrad.2018.03.013.
12. M. Ovreiu, D. Simon, Biogeography-based optimization of neuro-fuzzy system parameters for diagnosis of cardiac disease, in *Proceedings of the 12th Annual Conference on Genetic and Evolutionary Computation*, (2010), 1235–1242. https://doi.org/10.1145/1830483.1830706.
13. M. Ali, M. F. Rani, A. H. Jahidin, M. F. Saaid, M. Z. H. Noor, Identification of cardio myopathy disease using hybrid multilayered perceptron network, *in 2012 IEEE Internatio nal Conference on Control System, Computing and Engineering*, IEEE, (2013), 23–27. https://doi.org/10.1109/ICCSCE.2012.6487109.
14. D. Alis, A. Guler, M. Yergin, O. Asmakutlu, Assessment of ventricular tachyarrhythmia in patients with hypertrophic cardiomyopathy with machine learning-based texture analysis of late gadolinium enhancement cardiac MRI, *Diagn. Interv. Imaging*, **101** (2020), 137–146. https://doi.org/10.1016/j.diii.2019.10.005.
15. S. Borkar, M. N. Annadate, Supervised machine learning algorithm for detection of cardiac disorders, in *2018 Fourth International Conference on Computing Communication Control and Automation (ICCUBEA)*, IEEE, (2018), 1–4.. https://doi.org/10.1109/ICCUBEA.2018.8697795.
16. P. P. Sengupta, Y. M. Huang, M. Bansal, A. Ashrafi, M. Fisher, K. Shameer, et al., Cognitive machine-learning algorithm for cardiac imaging, *Circ. Cardiovasc. Imaging*, **9** (2016), e004330. https://doi.org/10.1161/CIRCIMAGING.115.004330.
17. R. Begum, M. Ramesh, Detection of cardiomyopathy using support vector machine and artificial neural network, *Int. J. Comput. Appl.*, **133** (2016), 29–34. https://doi.org/10.5120/ijca2016908178.

18. J. H. Joloudari, H. Saadatfar, A. Dehzangi, S. Shamshirband, Computer-aided decision-making for predicting liver disease using PSO-based optimized SVM with feature selection, *Inf. Med. Unlocked*, **17** (2019), 100255. https://doi.org/10.1016/j.imu.2019.100255.
19. E. M. Green, R. Van Mourik, C. Wolfus, S. B. Heitner, O. Dur, M. J. Semigran, Machine learning detection of obstructive hypertrophic cardiomyopathy using a wearable biosensor, *NPJ Digit. Med.*, **2** (2019), 57. https://doi.org/10.1038/s41746-019-0130-0.
20. D. Y. Tsai, K. Kojima, Measurements of texture features of medical images and its ap plication to computer-aided diagnosis in cardiomyopathy, *Measurement*, **37** (2005), 284–292. https://doi.org/10.1016/j.measurement.2004.11.015.
21. S. Narula, K. Shameer, A. M. Salem Omar, J. T. Dudley, P. P. Sengupta, Machine-learning algorithms to automate morphological and functional assessments in 2D echocardiography, *J. Am. Coll. Cardiol.*, **68** (2016), 2287. https://doi.org/10.1016/j.jacc.2016.08.062.
22. Q. A. Rahman, L. G. Tereshchenko, M. Kongkatong, T. Abraham, M. R. Abraham, H. Shatkay, Utilizing ECG-based heartbeat classification for hypertrophic cardiomyopathy identification, *IEEE Trans. Nanobiosci.*, **14** (2015), 505–512. https://doi.org/10.1109/TNB.2015.2426213.
23. X. Shao, Y. Sun, K. Xiao, Y. Zhang, W. Zhang, Z. Kou, et al., Texture analysis of magnetic resonance T1 mapping with dilated cardiomyopathy: A machine learning approach, *Medicine*, **97** (2018), e12246. https://doi.org/10.1097/MD.0000000000012246.
24. G. Captur, W. Heywood, C. Coats, S. Rosmini, V. Patel, L. R. Lopes, et al., Identificati on of a multiplex biomarker panel for hypertrophic cardiomyopathy using quantitative pr oteomics and machine learning, *Mol. Cell. Proteomics*, **19** (2020), 114. https://doi.org/10.1 074/mcp.RA119.001586.
25. F. Ali, S. El-Sappagh, S. R. Islam, D. Kwak, A. Ali, M. Imran, et al., A smart healthcare monitoring system for heart disease prediction based on ensemble deep learning and feature fusion, *Inf. Fusion*, **63** (2020), 208–222. https://doi.org/10.1016/j.inffus.2020.06.008.
26. A. Baccouche, B. Garcia-Zapirain, C. Castillo Olea, A. Elmaghraby, Ensemble deep learning models for heart disease classification: A case study from Mexico, *Information*, **11** (2020), 207. https://doi.org/10.3390/info11040207.
27. T. Chokwijitkul, A. Nguyen, H. Hassanzadeh, S. Perez, Identifying risk factors for heart disease in electronic medical records: A deep learning approach, in *Proceedings of the BioNLP 2018 Workshop*, (2018), 18–27. https://doi.org/10.18653/v1/W18-2303.
28. Y. S. Su, T. J. Ding, M. Y. Chen, Deep learning methods in internet of medical things f or valvular heart disease screening system, *IEEE Internet Things J.*, **99** (2021), 1. https:// doi.org/10.1109/JIOT.2021.3053420.
29. S. S. Sarmah, An efficient IoT-based patient monitoring and heart disease prediction system using deep learning modified neural network, *IEEE Access*, **8** (2020), 135784–135797. https://doi.org/10.1109/ACCESS.2020.3007561.
30. S. A. Morris, K. N. Lopez, Deep learning for detecting congenital heart disease in the fetus, *Nat. Med.*, **27** (2021), 764–765. https://doi.org/10.1038/s41591-021-01354-1.
31. S. Narmadha, S. Gokulan, M. Pavithra, R. Rajmohan, T. Ananthkumar, Determination of various deep learning parameters to predict heart disease for diabetes patients, in *2020 International Conference on System, Computation, Automation and Networking (ICSCAN)*, IEEE, (2020), 1–6. https://doi.org/10.1109/ICSCAN49426.2020.9262317.

32. R. Bharti, A. Khamparia, M. Shabaz, G. Dhiman, S. Pande, P. Singh, Prediction of heart disease using a combination of machine learning and deep learning, *Comput. Intell. Neurosci.*, **2021** (2021), 8387680. https://doi.org/10.1155/2021/8387680.
33. J. M. Kwon, K. H. Kim, K. H. Jeon, J. Park, Deep learning for predicting in-hospital mortality among heart disease patients based on echocardiography, *Echocardiography*, **36** (2019), 213–218. https://doi.org/10.1111/echo.14220.
34. S. Sharma, M. Parmar, Heart diseases prediction using deep learning neural network mod el., *Int. J. Innovative Technol. Explor. Eng.*, **9** (2020), 2278–3075. https://doi.org/10.35940 /ijitee.C9009.019320.
35. R. Poplin, A. V. Varadarajan, K. Blumer, Y. Liu, M. V. McConnell, G. S. Corrado, et al., Prediction of cardiovascular risk factors from retinal fundus photographs via deep learning, *Nat. Biomed. Eng.*, **2** (2018) 158–164. https://doi.org/10.1038/s41551-018-0195-0.
36. M. Chetrit, M. G. Friedrich, The unique role of cardiovascular magnetic resonance imagi ng in acute myocarditis, *F1000Research*, **7** (2018), 1153. https://doi.org/10.12688/f1000res earch.14857.1.
37. M. D. Cornicelli, C. K. Rigsby, K. Rychlik, E. Pahl, J. D. Robinson, Diagnostic performance of cardiovascular magnetic resonance native T1 and T2 mapping in pediatric patients with acute myocarditis, *J. Cardiovasc. Magn. Reson.*, **21** (2019), 40–48. https://doi.org/10.1186/s12968-019-0550-7.
38. M. A. G. M. Olimulder, J. Van Es, M. A. Galjee, The importance of cardiac MRI as a diagnostic tool in viral myocarditis-induced cardiomyopathy, *Neth. Heart J.*, **17** (2009), 481–486. https://doi.org/10.1007/BF03086308.
39. C. Moenninghoff, L. Umutlu, C. Kloeters, A. Ringelstein, M. E. Ladd, A. Sombetzki, et al., Workflow efficiency of two 1.5 T MR scanners with and without an automated user interface for head examinations, *Acad. Radiol.*, **20** (2013), 721–730. https://doi.org/10.1016/j.acra.2013.01.004.
40. M. Khodatars, A. Shoeibi, N. Ghassemi, M. Jafari, A. Khadem, D. Sadeghi, et al., Deep learning for neuroimaging-based diagnosis and rehabilitation of autism spectrum disorder: a review, *Comput. Biol. Med.*, **139** (2021). https://doi.org/10.1016/j.compbiomed.2021.104949.
41. N. Q. K. Le, Q. T. Ho, E. K. Y. Yapp, Y. Y. Ou, H. Y. Yeh, DeepETC: a deep convolutional neural network architecture for investigating and classifying electron transport chain's complexes, *Neurocomputing*, **375** (2020), 71–79. https://doi.org/10.1016/j.neucom.2019.09.070.
42. J. N. Sua, S. Y. Lim, M. H. Yulius, X. Su, E. K. Y. Yapp, N. Q. K. Le, et al., Incorp orating convolutional neural networks and sequence graph transform for identifying multil abel protein lysine ptm sites, *Chemom. Intell. Lab. Syst.*, **206** (2020), 104171. https://doi. org/10.1016/j.chemolab.2020.104171.
43. N. Ghassemi, H. Mahami, M. T. Darbandi, A. Shoeibi, S. Hussain, F. Nasirzadeh, et al., Material recognition for automated progress monitoring using deep learning methods, preprint, arXiv:2006.16344.
44. A. Shoeibi, M. Khodatars, N. Ghassemi, M. Jafari, P. Moridian, R. Alizadehsani, et al., Epileptic seizure detection using deep learning techniques: a review, *Int. J. Environ. Res. Public Health*, **18** (2021), 5780. https://doi.org/10.3390/ijerph18115780.
45. L. Fu, B. Lu, B. Nie, Z. Peng, H. Liu, X. Pi, Hybrid network with attention mechanism for detection and location of myocardial infarction based on 12-lead electrocardiogram signals, *Sensors*, **20** (2020), 1020. https://doi.org/10.3390/s20041020.

46. Y. Le Cun, B. Boser, J. S. Denker, D. Henderson, R. E. Howard, W. Hubbard, et al., Handwritten digit recognition with a back-propagation network, in *Proceedings of the 2nd International Conference on Neural Information Processing*, (1990), 396–404. Available from: https://papers.nips.cc/paper/1989/file/53c3bce66e43be4f209556518c2fcb54-Paper.pdf.
47. A. Krizhevsky, I. Sutskever, G. E. Hinton, Imagenet classification with deep convolutional neural networks, *Adv. Neural Inf. Process. Syst.*, **25** (2012), 1097–1105. https://doi.org/10.1145/3065386.
48. K. Simonyan, A. Zisserman, Very deep convolutional networks for large-scale image recognition, *Comput. Sci.*, preprint, arXiv:14091556.
49. C. Szegedy, W. Liu, Y. Jia, P. Sermanet, S. Reed, D. Anguelov, et al., Going deeper with convolutions; in *2015 IEEE Conference on Computer Vision and Pattern Recognition (CVPR)*, (2015), 1–9. https://doi.org/10.1109/CVPR.2015.7298594.
50. K. He, X. Zhang, S. Ren, J. Sun, Deep residual learning for image recognition, in *2016 IEEE Conference on Computer Vision and Pattern Recognition (CVPR)*, (2016), 770–778. https://doi.org/10.1109/CVPR.2016.90.
51. S. Lawrence, C. L. Giles, T. Ah Chung, A. D. Back, Face recognition: a convolutional neural-network approach, *IEEE Trans. Neural Networks*, **8** (1997), 98–113. https://doi.org/10.1109/72.554195.
52. R. Alizadehsani, M. Roshanzamir, S. Hussain, A. Khosravi, A. Koohestani, M. H. Zangooei, et al., Handling of uncertainty in medical data using machine learning and probability theory techniques: A review of 30 years (1991-2020), *Ann. Oper. Res.*, (2021), 1–42. https://doi.org/10.1007/s10479-021-04006-2.
53. H. Shin, H. R. Roth, M. Gao, L. Lu, Z. Xu, I. Nogues, et al., Deep convolutional neural networks for computer-aided detection: CNN architectures, dataset characteristics and transfer learning, *IEEE Trans. Med. Imaging*, **35** (2016), 1285–1298. https://doi.org/10.1109/TMI.2016.2528162.
54. U. R. Acharya, H. Fujita, S. L. Oh, Y. Hagiwara, J. H. Tan, M. Adam, et al., Deep convolutional neural network for the automated diagnosis of congestive heart failure using ECG signals, *Appl. Intell.*, **49** (2019), 16–27. https://doi.org/10.1007/s10489-018-1179-1.
55. U. R. Acharya, H. Fujita, O. S. Lih, M. Adam, J. H. Tan, C. K. Chua, Automated detection of coronary artery disease using different durations of ECG segments with convolutional neural network, *Knowl. Based Syst.*, **132** (2017), 62–71. https://doi.org/10.1016/j.knosys.2017.06.003.
56. J. H. Tan, Y. Hagiwara, W. Pang, I. Lim, S. L. Oh, M. Adam, et al., Application of sta cked convolutional and long short-term memory network for accurate identification of CAD ECG signals, *Comput, Biol. Med.*, **94** (2018), 19–26. https://doi.org/10.1016/j.compbiomed.2017.12.023.
57. A. Shoeibi, N. Ghassemi, R. Alizadehsani, M. Rouhani, H. Hosseini-Nejad, A. Khosravi, et al., A comprehensive comparison of handcrafted features and convolutional autoencoders for epileptic seizures detection in EEG signals, *Expert Syst. Appl.*, **163** (2021), 113788. https://doi.org/10.1016/j.eswa.2020.113788.
58. K. Wagstaff, C. Cardie, S. Rogers, S. Schrödl, Constrained k-means clustering with background knowledge, (2001), 577–584. Available from: http://www.litech.org/~wkiri/Papers/wagstaff-kmeans-01.pdf.
59. A. K. Jain, Data clustering: 50 years beyond K-means, *Pattern Recognit. Lett.*, **31** (2010), 651–666. https://doi.org/10.1016/j.patrec.2009.09.011.

60. R. Alizadehsani, M. Roshanzamir, M. Abdar, A. Beykikhoshk, A. Khosravi, M. Panahiazar, et al., A database for using machine learning and data mining techniques for coronary artery disease diagnosis, *Sci. Data*, **6** (2019), 227. https://doi.org/10.1038/s41597-019-0206-3.
61. G. Muhammad, M. S. Hossain, COVID-19 and non-COVID-19 classification using multi-layers fusion from lung ultrasound images, *Inf. Fusion*, **72** (2021), 80–88. https://doi.org/10.1016/j.inffus.2021.02.013.
62. S. Hussain, G. Hazarika, Educational data mining model using rattle, *Int. J. Adv. Comput. Sci. Appl.*, **5** (2014). https://doi.org/10.14569/IJACSA.2014.050605.
63. E. Haghighat, R. Juanes, Sciann: A keras/tensorflow wrapper for scientific computations and physics-informed deep learning using artificial neural networks, *Comput. Methods Appl. Mech. Eng.*, **373** (2021), 113552. https://doi.org/10.1016/j.cma.2020.113552.
64. R. Kumar, W. Wang, J. Kumar, T. Yang, A. Khan, W. Ali, et al., An integration of blockchain and AI for secure data sharing and detection of CT images for the hospitals, *Comput. Med. Imaging Graph.*, **87** (2021), 101812. https://doi.org/10.1016/j.compmedimag.2020.101812.
65. R. Yamashita, J. Long, A. Saleem, D. L. Rubin, J. Shen, Deep learning predicts postsurgical recurrence of hepatocellular carcinoma from digital histopathologic images, *Sci. Rep.*, **11** (2021), 2047. https://doi.org/10.1038/s41598-021-81506-y.
66. F. V. Jensen, F. Jensen, An introduction to Bayesian networks, Springer, 2014. https://doi.org/10.1007/978-3-642-54157-5_5.
67. H. M. Afify, M. S. Zanaty, Computational predictions for protein sequences of COVID-19 virus via machine learning algorithms, *Med. Biol. Eng. Comput.*, **59** (2021), 1723–1734. https://doi.org/10.21203/rs.3.rs-34004/v2.
68. F. Gorunescu, Data Mining: Concepts, models and techniques, Springer, 2011. https://doi.org/10.1007/978-3-642-19721-5.
69. J. H. Joloudari, E. H. Joloudari, H. Saadatfar, M. GhasemiGol, S. M. Razavi, A. Mosavi, et al., Coronary artery disease diagnosis; ranking the significant features using a random trees model, *Int. J. Environ. Res. Public Health*, **17** (2020), 731. https://doi.org/10.3390/ijerph17030731.
70. I. Ruczinski, C. Kooperberg, M. LeBlanc, Logic regression, *J. Comput. Graph. Stat.*, **12** (2003), 475–511. https://doi.org/10.1198/1061860032238.
71. G. Jones, J. Parr, P. Nithiarasu, S. Pant, A proof of concept study for machine learning application to stenosis detection, *Med. Biol. Eng. Comput.*, 2021. https://doi.org/10.1007/s11517-021-02424-9.
72. L. Breiman, Random forests, *Mach. Learn.*, **45** (2001), 5−32. https://doi.org/10.1023/A:1010933404324.
73. I. Kindermann, C. Barth, F. Mahfoud, C. Ukena, M. Lenski, A. Yilmaz, et al., Update on myocarditis, *J. Am. Coll. Cardiol.*, **59** (2012), 779. https://doi.org/10.1016/j.jacc.2011.09.074.
74. T. S. Kafil, N. Tzemos, Myocarditis in 2020: advancements in imaging and clinical management, *JACC Case Rep.*, **2** (2020), 178–179. https://doi.org/10.1016/j.jaccas.2020.01.004.
75. A. Roos, Diagnosis of myocarditis at cardiac MRI: the continuing quest for improved tissue characterization, *Radiology*, **292** (2019), 618–619. https://doi.org/10.1148/radiol.2019191476.
76. F. Dominguez, U. Kühl, B. Pieske, P. Garcia-Pavia, C. Tschöpe, Update on myocarditis and inflammatory cardiomyopathy: reemergence of endomyocardial biopsy, *Revista Española Cardiología*, **69** (2016), 178–187. https://doi.org/10.1016/j.rec.2015.10.015.

77. C. Buttà, L. Zappia, G. Laterra, M. Roberto, Diagnostic and prognostic role of electrocardiogram in acute myocarditis: A comprehensive review, *Ann. Noninvasive Electrocardiol.*, **1** (2020), 1–10. https://doi.org/10.1111/anec.12726.
78. P. Bholowalia, A. Kumar, EBK-means: A clustering technique based on elbow method and k-means in WSN, *Int. J. Comput. Appl.*, **105** (2014), 17–24. https://doi.org/10.5120/18405-9674.

Appendix

In order to find the best number of clusters, the Elbow method was used. In this method, different values of K (from 1 to 30) were investigated. Figure A.1 shows the result to identify the optimal K. As shown in this figure since we did not observe a sharp elbow, the exact amount of the best K was not determined using this method.

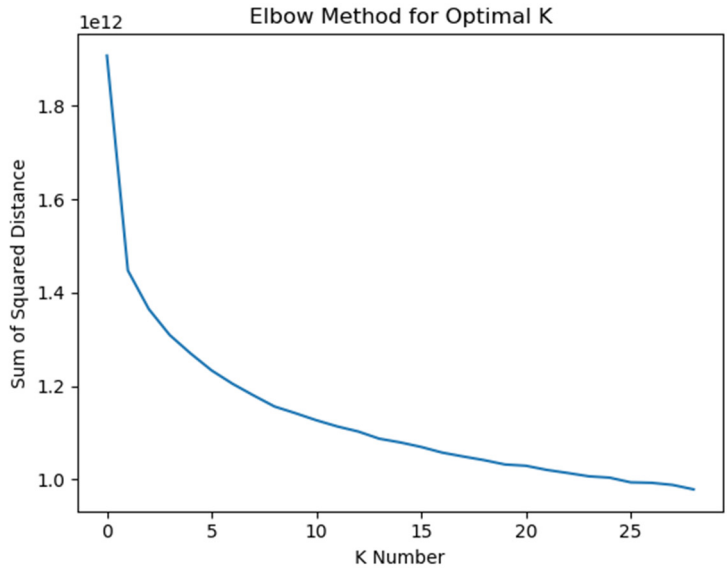

Figure A.1. Results for elbow method for different values of K.